BIOCHEMISTRY
including biophysical chemistry & molecular biology

Article

pubs.acs.org/biochemistry

Solution Structure of Calmodulin Bound to the Target Peptide of Endothelial Nitric Oxide Synthase Phosphorylated at Thr495

Michael Piazza, Valentina Taiakina, Simon R. Guillemette, J. Guy Guillemette,* and Thorsten Dieckmann*

Department of Chemistry, University of Waterloo, Waterloo, Ontario N2L 3G1, Canada

Supporting Information

ABSTRACT: Nitric oxide synthase (NOS) plays a major role in a number of key physiological and pathological processes, and it is important to understand how this enzyme is regulated. The small acidic calcium binding protein, calmodulin (CaM), is required to fully activate the enzyme. The exact mechanism of how CaM activates NOS is not fully understood at this time. Studies have shown CaM to act like a switch that causes a conformational change in NOS to allow for the transfer of an electron between the reductase and oxygenase domains through a process that is thought to be highly dynamic and at least in part controlled by several possible phosphorylation sites. We have determined the solution structure of CaM bound to a peptide that contains a phosphorylated threonine corresponding to Thr495 in full size endothelial NOS (eNOS) to investigate the structural and functional effects that the phosphorylation of this residue may have on nitric oxide production. Our biophysical studies show that phosphorylation of Thr495 introduces electrostatic repulsions between the target sequence and CaM as well as a diminished propensity for the peptide to form an α-helix. The calcium affinity of the CaM−target peptide complex is reduced because of phosphorylation, and this leads to weaker binding at low physiological calcium concentrations. This study provides an explanation for the reduced level of NO production by eNOS carrying a phosphorylated Thr495 residue.

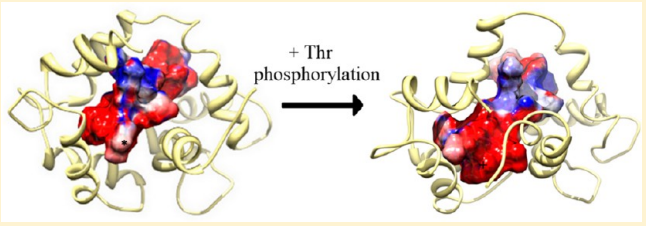

Nitric oxide synthase (NOS) enzymes (EC 1.14.13.39) catalyze the production of nitric oxide (•NO) that acts as a secondary inter- and intracellular messenger involved in many physiological processes.[1] Three NOS isozymes are found in mammals: neuronal NOS (nNOS or NOS I), endothelial NOS (eNOS or NOS III), and inducible NOS (iNOS or NOS II). The NOS enzymes are homodimeric, with each monomer containing an N-terminal oxygenase domain, which contains binding sites for the catalytic heme, tetrahydrobiopterin (H_4B), and the substrates L-arginine and molecular oxygen, and a C-terminal reductase domain, which contains binding sites for cofactors FMN, FAD, and NADPH. A calmodulin (CaM) binding domain connects the oxygenase and reductase domains and is required for the efficient transfer of an electron from the reductase to the oxygenase domain for •NO production.[1,2] CaM binds and activates the Ca^{2+}-dependent constitutive NOS (cNOS) enzymes, eNOS and nNOS, at elevated cellular Ca^{2+} concentrations, whereas iNOS is transcriptionally controlled *in vivo* by cytokines and binds to CaM in a Ca^{2+}-independent manner. A large conformational change that CaM induces in the reductase domain of the NOS enzymes allows the FMN domain to interact with the FAD to accept electrons and pass the electrons to the heme during catalysis.[3] Clearly, these conformational changes caused by CaM are important in stimulating efficient electron transfer within the NOS enzymes.

CaM is a ubiquitous cytosolic Ca^{2+}-binding protein that is able to bind and regulate hundreds of different intracellular proteins.[4] CaM consists of two globular domains joined by a flexible central linker region. Each domain contains two EF hand pairs that are each capable of binding one Ca^{2+} ion. The binding of Ca^{2+} to CaM causes a conformational change that exposes hydrophobic patches that allow it to associate with its intracellular target proteins. The flexibility of CaM's central linker separating the N- and C-domains allows it to adapt its conformation to optimally associate with its intracellular targets.[5,6] Both the N- and C-lobes must be calcium replete to fully activate eNOS and nNOS enzymes.[7,8]

eNOS activity is regulated by multiple mechanisms, including posttranslational modifications such as protein phosphorylation.[9,10] The binding of CaM and the transfer of electrons from the reductase to the oxygenase domain of eNOS are dependent on protein phosphorylation and dephosphorylation.[9] eNOS can be phosphorylated on serine, tyrosine, and threonine residues and contains many potential phosphorylation sites that can play a role in regulating its activity.[11−14] Phosphorylation of Ser1177 in the reductase domain has been found to result in the activation of eNOS, whereas phosphorylation of Thr495 within the CaM-binding domain has been found to reduce eNOS activity.[15−17] Perturbations of eNOS phosphorylation have been reported in a number of diseases.[18] Phosphorylation of Thr495 acts as a negative regulatory site and has been reported to interfere with the binding of CaM to the CaM-binding domain affecting activation of the enzyme.[9,15]

Received: October 28, 2013
Revised: December 3, 2013
Published: February 4, 2014

   dx.doi.org/10.1021/bi401466s | *Biochemistry* 2014, 53, 1241−1249

There is considerable interest in understanding the structural and functional effects that the phosphorylation of Thr495 in eNOS has on the calcium-dependent CaM binding and activation of the enzyme. In this study, the structural and functional effects that the phosphorylation of eNOS has on binding to CaM were investigated. Steady-state fluorescence and isothermal titration calorimetry (ITC) were used to monitor the binding of CaM to the wild-type eNOS CaM-binding region peptide and the eNOS CaM-binding region peptide phosphorylated at Thr495 at various free Ca^{2+} concentrations. The structural effects of Thr495 phosphorylation on the binding of CaM to eNOS were investigated by the determination of the solution structure of CaM bound to the eNOS CaM-binding region peptide phosphorylated at Thr495. This investigation provides a better understanding of the interaction of CaM with the phosphorylated or non-phosphorylated CaM-binding region of eNOS at Thr495.

EXPERIMENTAL PROCEDURES

CaM Protein Expression and Purification. Wild-type CaM protein was expressed and purified using phenyl-Sepharose chromatography, as previously described.[7] Isolation of the CaM proteins (148 residues) was confirmed by electrospray ionization mass spectrometry (ESI-MS), and purity was judged to be >95% by sodium dodecyl sulfate−polyacrylamide gel electrophoresis. The human eNOS (TRKKTFKEVANAVKISASLMGT, 22 residues corresponding to residues 491−512 from the full-length eNOS protein) peptide was synthesized and purchased from Sigma. The Thr495-phosphorylated human eNOS (TRKKpTFKEVANAVKISASLM, 20 residues corresponding to residues 491−510 from the full-length eNOS protein) peptide was synthesized and purchased from GenScript. The phosphorylation was confirmed by ESI-MS.

Sample Preparation for the NMR Investigation. CaM for NMR experiments was expressed in M9 medium (11.03 g/L $Na_2HPO_4{\cdot}7H_2O$, 3.0 g/L KH_2PO_4, 0.5 g/L NaCl, 2 mM $MgSO_4$, 0.1 mM $CaCl_2$, 5 mg/mL thiamine, and 100 μg/mL kanamycin) containing 2 g/L [^{13}C]glucose and 1 g/L $^{15}NH_4Cl$. [^{13}C,^{15}N]CaM was purified as described above. The samples were prepared for NMR experiments via exchange of a buffer into NMR solution (100 mM KCl, 10 mM $CaCl_2$, 0.2 mM NaN_3, and a 90% H_2O/10% ^2H_2O mixture) at pH 6.0 using a YM10 centrifugal filter device (Millipore Corp., Billerica, MA). All NMR samples contained at least 1 mM CaM in a total volume of 500 μL. The samples were transferred into 5 mm NMR sample tubes and stored at 4 °C until they were required for NMR experiments. NMR experiments on the complexes were conducted on CaM samples titrated with the eNOSpT495 peptide to saturation in a 1:1 CaM:peptide ratio. Complex formation was monitored after each addition by acquisition of a ^{1}H−^{15}N heteronuclear single-quantum coherence (HSQC) spectrum.

NMR Spectroscopy and Data Analysis. NMR spectra were recorded at 25 °C on Bruker 600 and 700 MHz DRX spectrometers equipped with XYZ-gradient triple-resonance probes (Bruker, Billerica, MA). Spectra were analyzed using CARA (Computer Aided Resonance Assignment).[19]

Specific assignments of the CaM backbone resonances were achieved using a combination of three-dimensional triple-resonance experiments, including HNCA, HN(CO)CA, CBCA(CO)NH, and HNCO.[20,21] Side chain resonances were assigned using TOCSY-type experiments HC(C)H-TOCSY, (H)CCH-TOCSY, and H(CCO)NH.[22] Specific assignments of the eNOSpThr495 peptide were obtained from ^{15}N-double-filtered NOESY experiments (Figure S1 of the Supporting Information).[23]

Structure Calculation. The ^{1}H, ^{13}C, and ^{15}N resonance assignments were utilized to identify constraints for the structure calculations. Distance constraints for the solution structure of the CaM−eNOSpThr495 complex were obtained from ^{15}N NOESY-HSQC, ^{13}C NOESY-HSQC, and ^{15}N-double-filtered NOESY spectra acquired on samples containing labeled CaM and unlabeled peptide.[23−25] In addition, dihedral angle restraints were derived from chemical shift analysis with TALOS+.[26] CNSsolve version 1.2[27] was used to perform the structure calculations using standard simulated annealing protocols.

Delphi Calculation of the CaM Structures. Delphi electrostatic potentials of the structure were calculated using the DelphiController interface of UCSF Chimera version 1.5.3 (build 33475).[28] The parseRes atomic radius file and atomic charge file were used as the input files in the calculation. The electrostatic potential surface was visualized in Chimera.

Dansylation of CaM. Dansyl-CaM was prepared as previously described.[29] CaM (1 mg/mL) was buffer exchanged into 10 mM $NaHCO_3$ and 1 mM EDTA (pH 10.0) at 4 °C. Thirty microliters of 6 mM dansyl chloride (1.5 mol/mol of CaM) in DMSO was added to 2 mL of CaM, while it was being stirred. After incubation for 12 h at 4 °C, the mixture was first exhaustively dialyzed against 500 volumes of 150 mM NaCl, 1 mM EDTA, and 20 mM Tris-HCl (pH 7.5) at 4 °C and then exhaustively dialyzed against 500 volumes of water. Labeling yields were determined from absorbance spectra using an ε_{320} of 3400 M^{-1} cm^{-1} and were compared to actual protein concentrations determined using the Bradford method with wild-type CaM used as the protein standard.[30] ESI-MS was used to confirm successful dansyl labeling of each CaM protein. The concentration of dansyl-CaM in all experiments was 2 μM.

Steady-State Fluorescence. Fluorescence emission spectra were recorded using a PTI (London, ON) QuantaMaster spectrofluorimeter. Fluorescence measurements were taken on 50 μL samples consisting of dansyl-CaM (2 μM) alone or with eNOS or eNOSpThr495 peptide in 30 mM MOPS, 100 mM KCl, and 10 mM EGTA (pH 7.2) with an increasing concentration of free Ca^{2+}. The free Ca^{2+} concentration was controlled using the suggested protocol from the calcium calibration buffer kit from Invitrogen. The excitation wavelength for all of the dansyl-CaMs was set to 340 nm, and emission was monitored between 400 and 600 nm. Slit widths were set at 2 nm for excitation and 1 nm for emission. The relative fluorescence was calculated with the equation relative fluorescence = $(F - F_0)/(F_{max} - F_0)$, where F is the measured intensity, F_{max} is the maximal intensity, and F_0 is the intensity without added Ca^{2+}.

Isothermal Titration Calorimetry (ITC). All ITC recordings were performed on a Microcal ITC200 instrument from Microcal (Northampton, MA) at 25 °C with a stir speed of 1000 rpm and the reference power set to 5 μcal/s. In the experiments at saturating Ca^{2+} concentrations, the buffer consisted of 30 mM MOPS, 100 mM KCl (pH 7.2), and 1 mM $CaCl_2$ and was identical between the cell and syringe. In the experiments at 225 nM free Ca^{2+}, the calcium calibration buffer kit from Invitrogen was used and the buffer consisted of 15 mM MOPS, 50 mM KCl (pH 7.2), 10 mM EGTA, and 6.0 mM CaEGTA and was identical between the cell and syringe.

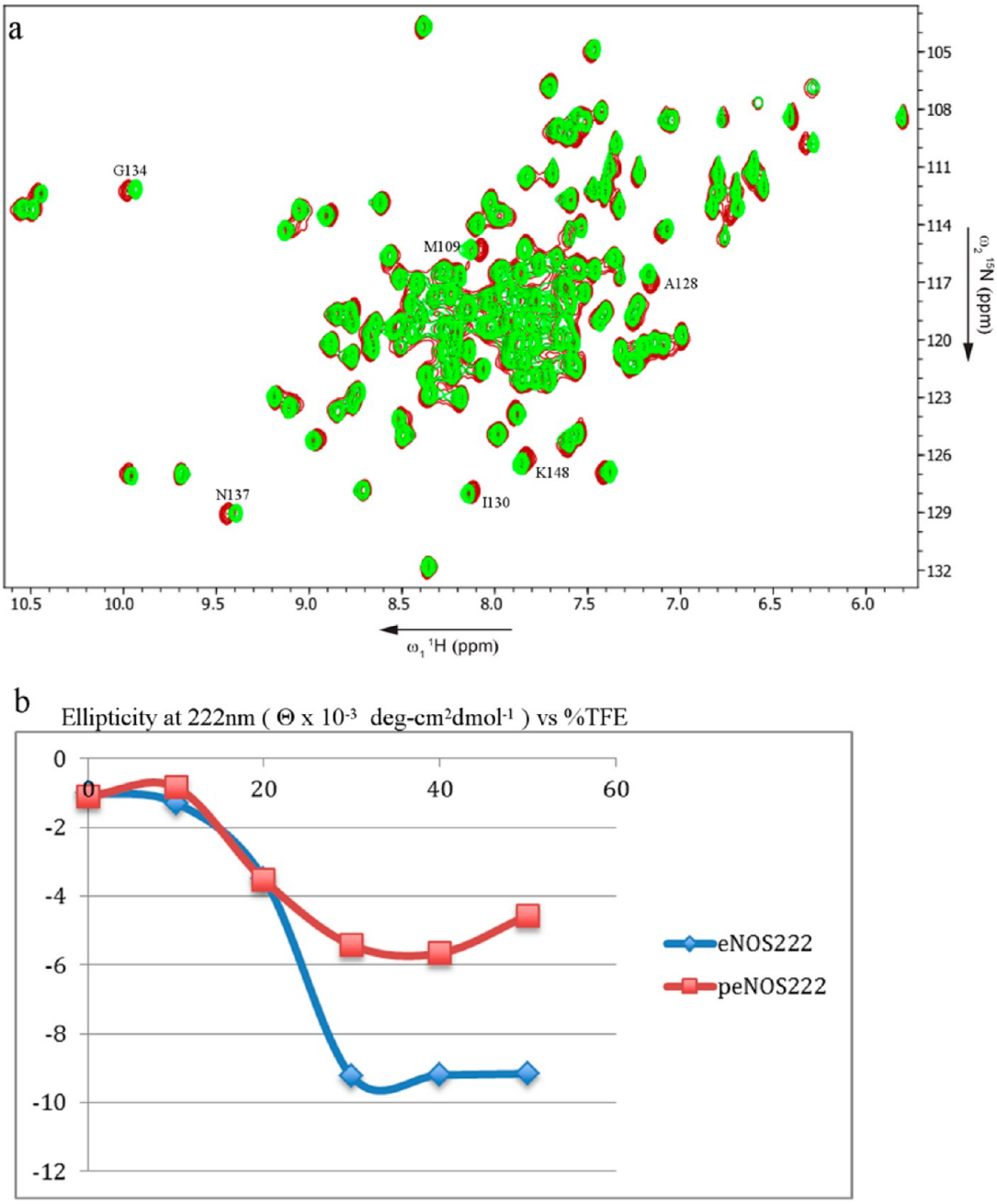

Figure 1. (a) Overlay of $^{1}H-^{15}N$ HSQC spectra of the CaM–eNOS peptide complex (green) and the CaM–eNOSpThr495 peptide complex (red). (b) Comparison of UV–CD spectra between wild-type eNOS and eNOSpThr495 CaM-binding peptides in buffers with varying TFE concentrations. The ellipticiy at 222 nm is shown as a function of TFE concentration.

Buffer into buffer, peptide into buffer, and buffer into CaM controls showed no significant baseline decay or drift and relatively low consistent heats of injection, indicating sufficiently matched cell and syringe buffer conditions; 39 μL of each peptide was titrated into 200 μL of CaM at varying concentrations (optimal starting conditions were determined empirically), typically from 100 μM peptide into 10 μM CaM to 500 μM peptide into 50 μM CaM, over the course of 20–30 injections at 2–3 min intervals. Data analysis was performed using the Origin ITC200 Origin70 module with preloaded fitting equations for one- and two-site models. The one-set-of-sites model was found to be applicable to all experiments.

Circular Dichroism (spectropolarimetry). CD was assessed using a Jasco J-715 CD spectropolarimeter and analyzed using J-715 software (Jasco Inc., Easton, MD) as previously described[8] with some modifications. Samples were measured in a 1 mm quartz cuvette (Hellma, Concord, ON) and kept at 25 °C using a Peltier-type constant-temperature cell holder (model PFD 3505, Jasco Inc.). Samples consisted of 10 μM synthetic eNOS or phosphorylated eNOS (peNOS) CaM-binding domain peptides. Samples were in 10 mM Tris-HCl buffer (pH 7.5), 150 mM NaCl, and 200 μM $CaCl_2$. Spectra were recorded over the range of 190–250 nm with a 1.0 nm bandwidth, a 0.2 nm resolution, a 100 mdeg sensitivity at a 0.125 s response, and a rate of 100 nm/min with a total of 25 accumulations. Data are expressed as the mean residue ellipticity (θ) in degrees square centimeters per decimole.

dx.doi.org/10.1021/bi401466s | *Biochemistry* 2014, 53, 1241–1249

Accession Numbers. The coordinates and NMR parameters have been deposited in the Protein Data Bank (PDB) and the BioMagResBank (BMRB) and have been assigned RCSB ID code rcsb103588, PDB entry 2mg5, and BMRB accession number 19586.

RESULTS AND DISCUSSION

CD and NMR Spectroscopy. NMR spectroscopy was used to assess changes to the CaM−eNOS complex due to the phosphorylation of Thr495. Figure 1a shows the overlay of the ^{15}N HSQC spectra of the CaM−eNOS complex with that of the CaM−eNOSpThr495 complex. Cross-peaks for the majority of amides in the CaM−eNOSpThr495 complex overlap with those of the CaM−eNOS complex. However, amides in the C-domain, specifically the amides of residues in EF hand IV, do not overlap with those of the CaM−eNOS complex because of differences in chemical shifts. Also not seen in Figure 1a is the chemical shift difference of E7, which is located in the heavily overlapped central portion of the spectra. These data suggest that the structures of the CaM−eNOS complex and the CaM−eNOSpThr495 complex are quite similar. This provides further evidence that this phosphorylation affects residues E7 and E127, which are in the proximity of the phosphorylated Thr495 in the structure. This has been previously postulated by Aoyagi et al., who suggested that the addition of a negatively charged phosphate group would cause electrostatic repulsion between E7 and E127.[31]

The effect of phosphorylation on the secondary structure of the peptide was investigated using trifluoroethanol (TFE) monitored by circular dichroism spectroscopy. The TFE is used to mimic hydrophobic environments and is known to induce an α-helical conformation in peptides that have a propensity to form this secondary structure. Both eNOS peptides showed no apparent structure in the buffer solution with 0% TFE. A comparison of the tendency of each peptide to form an α-helix was then performed by recording spectra after the addition of increasing concentrations of TFE. The formation of an α-helix is generally accompanied by the appearance of negative ellipticity at 208 and 222 nm. Both peptides showed increased amounts of secondary structure as more TFE was added. In both cases, there was an increase in the level of apparent α-helical structure with an increase in TFE concentration. With increasing TFE concentrations, the negative ellipticity at 222 nm of both peptides plateaus at TFE concentrations of >30% (see Figure 1b). While this result indicates that the increase in the level of helical structure does not appreciably change above 30% TFE, the phosphorylated peptide did not show an α-helical content as large as that of the nonphosphorylated peptide (Figure 1b). The structural effects of the phosphorylation leading to the diminished level of helical structure of the peptide can be due to the charged and bulky nature of the phosphate, destabilization of electrostatics that can result in nonproductive interaction with neighboring residues, or the high desolvation penalty of the side chain.[32] Specifically, it has been previously proposed that phosphorylation at Thr495 OG1 would disrupt its hydrogen bond with the Glu498 backbone amide, possibly affecting the α-helical secondary structure of the peptide.[31] In addition, Thr495 is next to one of the anchoring residues in the classical "1-5-8-14" CaM-binding sequence motif. A negatively charged phosphorylated Thr495 next to the first residue of the motif will likely disrupt the helical structure of the region.

While the propensity of the phosphorylated eNOS CaM-binding domain to form an α-helix appears to be diminished, the final structure of the peptide bound to CaM is very similar to that of the nonphosphorylated form of the peptide. The diminished α-helical propensity could account for the reduced activity of the enzymes associated with the phosphorylated form.

Structure of the CaM−eNOSpThr495 Complex. The three-dimensional solution structure of CaM bound to the human eNOS CaM-binding domain peptide phosphorylated at Thr495 (CaM−eNOSpThr495) was determined using multidimensional heteronuclear NMR spectroscopy. The structure of the complex is based on a large number of experimental constraints and is well-defined. Structure and input data statistics are summarized in Table 1. The family of 20 final structures is shown in Figure 2a. The average structure showing the location of the phosphorylation of Thr495 of the eNOS peptide, which is found near the N-terminal end of the peptide, is shown in Figure 2b. Residues 1−4 (corresponding to residues 491−494 of eNOS) at the N-terminus of the eNOSpThr495 CaM-binding region peptide were not included in the structure calculation because they could not be unambiguously assigned. This could be due to the addition of the phosphate group that has been theorized to destabilize the helical propensity of the peptide.[31] On the basis of the comparison of the ^{15}N-double-filtered NOESY experiments for CaM with the eNOS peptide and CaM with the eNOSpThr495 peptide, there was little change in the chemical shifts observed for pThr495 and Thr495.

Table 1. Statistics for the CaM−eNOSpThr495 Peptide Structural Ensemble

NMR-Derived Distance and Dihedral Angle Restraints			
	calmodulin	eNOSphos peptide	CaM−eNOSphos complex
NOE constraints			
total	1513	119	62
dihedral angles from TALOS+	288	N/A	N/A
total no. of restraints	1982		

Structure Statistics for the 20 Lowest-Energy Structures			
mean deviation from ideal covalent geometry			
bond lengths (Å)		0.010	
bond angles (deg)		1.3	
	all residues	ordered residues[a]	selected residues[b]
average pairwise rmsd (Å) for all heavy atoms of the 20 lowest-energy structures			
backbone atoms	1.3	0.9	0.9
heavy atoms	1.7	1.4	1.4
Ramachandran statistics (%)			
residues in most favored region		86.0	
residues in additional allowed regions		13.5	
residues in generously allowed region		0.4	
residues in disallowed region		0.0	

[a]Ordered residue ranges: 6A−8A, 10A−36A, 39A−77A, 79A−148A, and 495B−508B. [b]Selected residue ranges: 6A−8A, 10A−36A, 39A−77A, 79A−148A, 495B−508B.

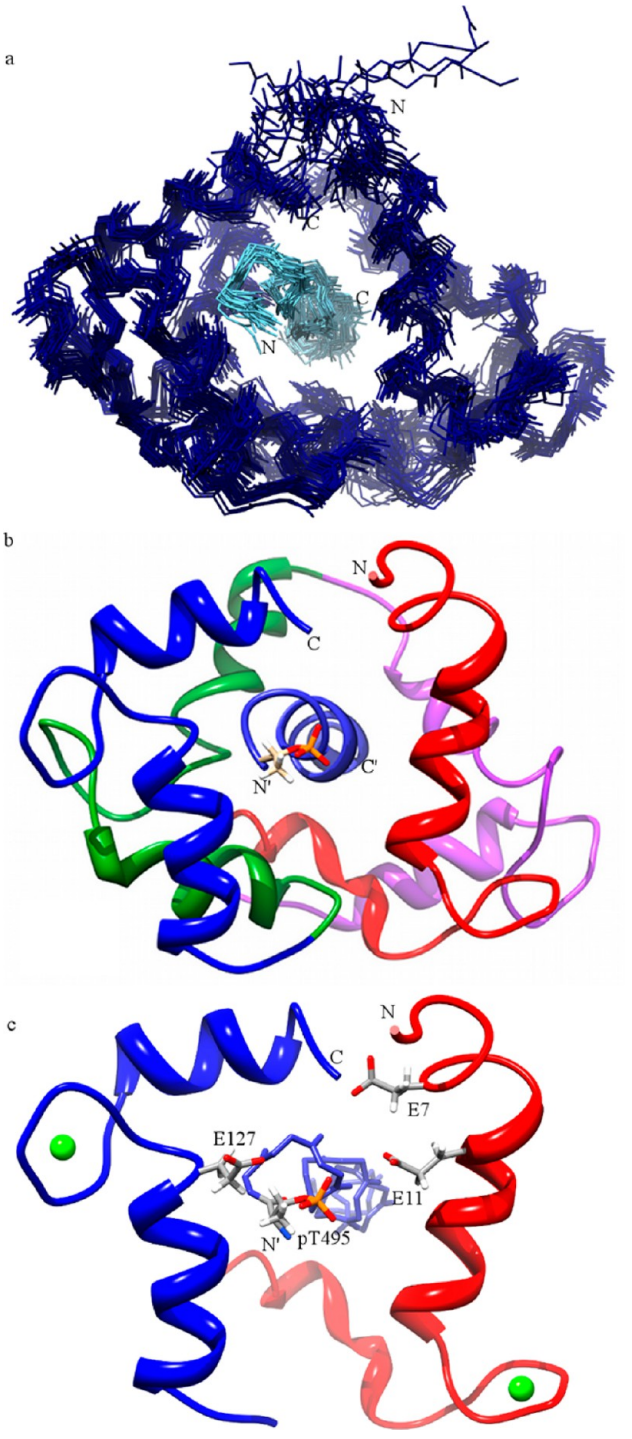

Figure 2. Solution structure of CaM bound to the eNOSpThr495 CaM-binding domain peptide. (a) Superposition of the ensemble of the 20 lowest-energy structures of CaM bound to the eNOSpThr495 peptide. Backbone atom traces of CaM are colored dark blue, and those of the eNOSpThr495 peptide are colored light blue. (b) Cartoon ribbon view of the average solution structure of the CaM–eNOSpThr495 complex. (c) Cartoon ribbon view showing residues in the proximity of the phosphorylated Thr495 of the eNOS peptide. Ca^{2+} ions are shown as green dots and are modeled in their known locations. Residues 1–40 of CaM (EF hand I) are colored red, residues 41–79 (EF hand II) purple, residues 80–114 (EF hand III) green, and residues 115–148 (EF hand IV) blue. The peptide is colored lighter blue, and the N- and C-termini are labeled N′ and C′, respectively. The phosphorylated threonine is shown as a stick model.

Comparison of the CaM–eNOS and CaM–eNOSpThr495 Complexes. When the solution structure of the CaM–eNOS complex is superimposed on that of the CaM–eNOSpThr495 complex, the two structures are shown to be quite similar; however, a few local differences are seen (Figure 3). When they are aligned with respect to the backbone atoms of the peptide, a difference is shown in the orientation of helix A of CaM between the two structures, with helix A of the CaM–eNOSpThr495 complex being pushed away from the N-terminus of the peptide (where the phosphorylated Thr495 is located). EF hand IV (colored blue) is also shifted farther from the peptide in the structure of the CaM–eNOSpThr495 complex. The rest of the structure of the CaM–eNOSpThr495 complex superimposes quite well on the structure of the CaM–eNOS complex. This, along with the ^{15}N HSQC spectra overlay, confirms that the phosphorylation of Thr495 does not have an effect on the structure of CaM away from the site of phosphorylation.

Electrostatic Effects of the Phosphorylation of Thr495. The addition of the phosphate group to Thr495 of the eNOS peptide shows structural effects on EF hands I and IV. This is first illustrated by the overlay of the ^{15}N HSQC spectra of the CaM–eNOS and CaM–eNOSpThr495 complexes (Figure 1a) and is clearly shown by the structural overlay of the two structures (Figure 3). The analysis of the structure of the CaM–eNOSpThr495 complex with Delphi illustrates that this modification to the peptide creates a more negative potential on the N-terminal region of the peptide, which is located in a negatively charged region of CaM (Figure 4b,d). This negative charge is not present in the CaM–eNOS complex (Figure 4c) and thus would not cause any electrostatic repulsion. This phosphate group is in the proximity of E7, which is found in helix A of EF hand I, and E127, which is found in helix G of EF hand IV. The electrostatic repulsion between the phosphate group and helix A of EF hand I gives an explanation of why helix A is pushed farther from the peptide in the CaM–eNOSpThr495 complex, as shown in Figure 3. This also explains why helix G and EF hand IV are shifted farther from the eNOSpThr495 peptide. This electrostatic repulsion could be affecting CaM's ability to coordinate Ca^{2+} by interfering with EF hands I and IV, which would help explain why CaM has a weakened ability to bind eNOS phosphorylated at Thr495 at physiological Ca^{2+} levels.

Fluorescence Spectroscopy Suggests Increased Ca^{2+} Sensitivity of CaM with the eNOS Peptide. Binding of the eNOS and eNOSpThr495 peptides with CaM was further studied using dansylated CaM (dansyl-CaM). Dansyl-CaM is a useful tool for detecting conformational changes in CaM as a result of interactions with Ca^{2+}, peptides, or other proteins because the intensity of the fluorescence spectrum is enhanced and shifted when the dansyl moiety becomes embedded in a hydrophobic environment.[29,33] Without Ca^{2+} present, there was no blue shift or enhancement of the dansyl fluorescence spectrum observed when the eNOS peptide or eNOSpThr495 peptide was added. In the presence of Ca^{2+}, this shift and enhancement of the fluorescence spectrum was observed. To analyze the Ca^{2+} dependency of the two complexes, we performed Ca^{2+} titration fluorescence experiments in triplicate (Figure 5). Without peptides, dansyl-CaM exhibited fluorescence changes in a Ca^{2+} concentration range of 0.35–2.8 μM. The fluorescence changes of the dansyl-CaM–eNOS complex occurred over a much lower Ca^{2+} concentration range, which may correspond to a physiological Ca^{2+} concentration. The

dx.doi.org/10.1021/bi401466s | *Biochemistry* 2014, 53, 1241–1249

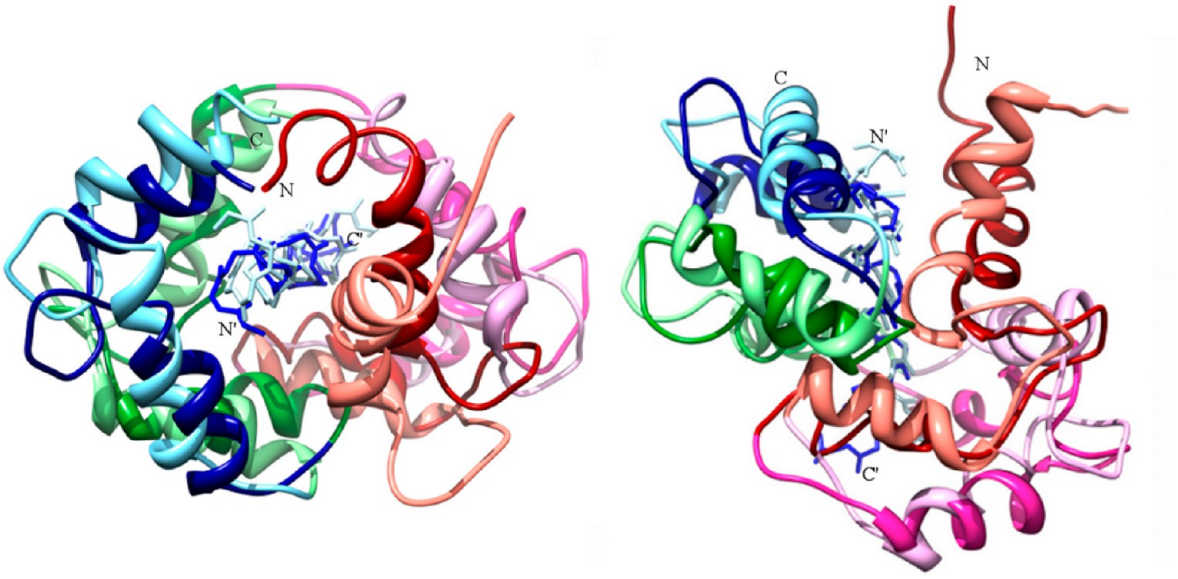

Figure 3. Superpositions of the CaM−eNOS peptide solution structure (dark colors) and the CaM−eNOSpThr495 peptide solution structure (light colors). Comparison of solution structures of the CaM−eNOSpThr495 peptide (dark colors) and CaM−eNOS peptide complexes by superimposition of the two structures viewed along the bound peptide from its N-terminus (N′) to its C-terminus (C′) (left, front view) and rotated 90° around the horizontal axis with the N-terminus of the bound peptide on the top (right, bottom view). The two structures are aligned by superimposing backbone atoms of the bound peptides. The color scheme is the same as that in Figure 1.

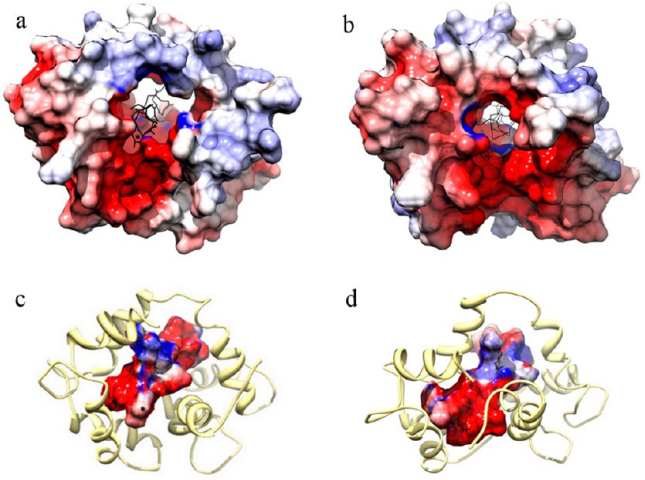

Figure 4. Delphi-calculated electrostatic potential maps are projected on the surface of the CaM−eNOS peptide complex (a and c) and the CaM−eNOSpThr495 peptide complex (b and d). Thr495 and pThr495 are denoted on the peptide with asterisks and plus signs, respectively. The Delphi-calculated electrostatic potential maps are colored with a chimera color key ranging from red (−15) to blue (0).

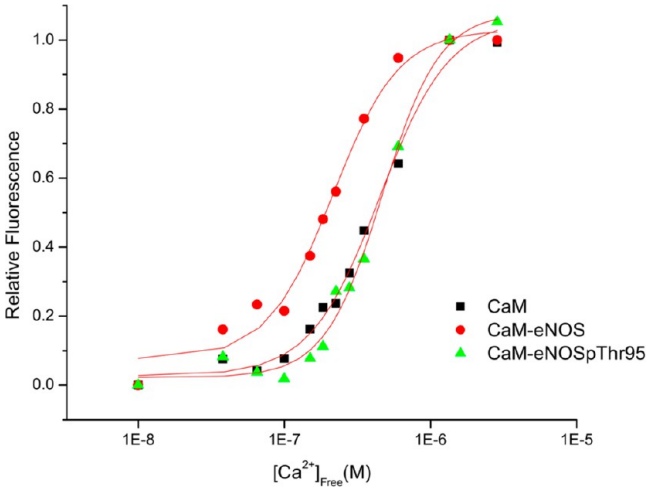

Figure 5. Ca^{2+} dependency of dansyl-CaM fluorescence with or without eNOS and eNOSpThr495 peptides. The normalized fluorescence is shown for CaM, the CM−eNOS complex, and the CaM−eNOSpThr495 complex under assay conditions described in Experimental Procedures.

dansyl-CaM−eNOSpThr495 complex showed no difference in Ca^{2+} dependency when compared to CaM alone. These Ca^{2+} titration experiments provide information about the conformational transitions of CaM with the peptides and Ca^{2+}. The finding that the CaM−eNOS complex binds with Ca^{2+} at Ca^{2+} concentrations lower than those with CaM alone indicates that the Ca^{2+} affinity of CaM is enhanced with the peptide binding to CaM. This is not seen in the interaction of CaM with the eNOSpThr495 peptide. This increased Ca^{2+} sensitivity of CaM has also been seen with other peptides interacting with CaM.[34] This suggests that binding of the eNOS peptide to CaM increases the Ca^{2+} sensitivity of CaM in the physiological Ca^{2+} concentration range, whereas eNOSpThr495 does not.

Isothermal Titration Calorimetry (ITC). ITC was used to examine the thermodynamic profiles associated with the binding of CaM to the two target peptides. Because the values obtained for binding constants show slight variations when experiments are performed using different methods and conditions,[35,36] all of our experiments were performed by ITC using exactly the same conditions. Representative titrations for each are shown in Figure 6. In the presence of excess calcium (1 mM), the wild-type eNOS peptide binds to CaM by an exothermic interaction. As previously reported for the binding of the nNOS peptide,[37] eNOS binding proceeds with a negative enthalpy (ΔH), a positive entropy (ΔS), and a modest affinity (K_d = 0.7 μM) (Table 2). This indicates that the interaction is driven by favorable enthalpy and entropy. In

dx.doi.org/10.1021/bi401466s | *Biochemistry* 2014, 53, 1241−1249

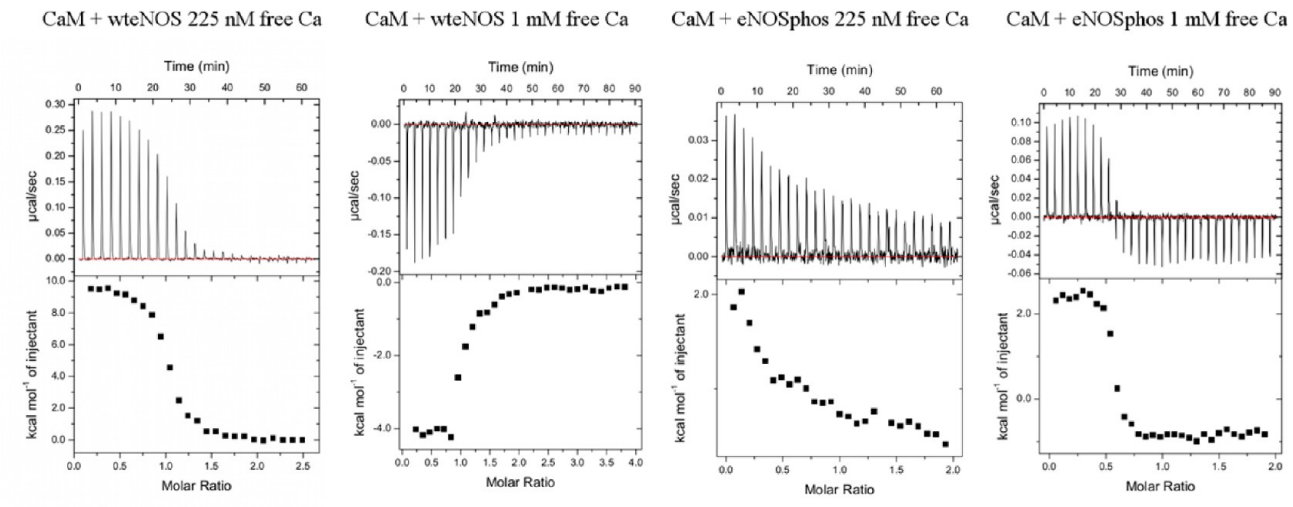

Figure 6. ITC analysis indicates binding of the eNOS peptide and no binding of the eNOSpThr495 peptide to CaM at physiological Ca^{2+} levels. Representative raw sample data for several CaM−peptide titrations.

Table 2. Thermodynamics of CaM−Peptide Interactions Measured by ITC

	N (sites)	K_d (μM)	ΔH (kcal/mol)	ΔS (cal mol^{-1} K^{-1})
CaM−eNOS with 0.225 μM free Ca^{2+}	1.00 ± 0.01	0.2 ± 0.03	9.39 ± 0.13	62.0
CaM−eNOS with 1 mM free Ca^{2+}	1.02 ± 0.02	0.7 ± 0.2	−4.48 ± 0.16	13.3
CaM−eNOSpThr495 with 0.225 μM free Ca^{2+}	0.0096 ± 0.86[a]	>50	41.07 ± 369.9[a]	140[a]
CaM−eNOSpThr495 with 1 mM free Ca^{2+}	1.11 ± 0.01	0.3 ± 0.08	1.74 ± 0.03	35.5

[a]These results cannot be fit reliably by the ITC software and are indicative of poor or no binding between CaM and the eNOSpThr495 peptide.

contrast, the binding of the eNOSpThr495 peptide under the same conditions is weakly endothermic, with an affinity comparable to that of the wild type (K_d = 0.3 μM). A similar endothermic interaction has been reported for apoCaM titrated with mutant peptides corresponding to the CaM-binding domain of iNOS, an isoform that is known to bind to CaM in the absence of calcium.[38] The eNOSpThr495 binding interaction proceeds with positive ΔH and ΔS values. The interaction is therefore driven by the increase in entropy. Both peptides showed a 1:1 stoichiometry with CaM as expected.

Because our fluorescence studies showed an apparent difference in binding at low calcium concentrations, we attempted to thermodynamically characterize the interactions under these conditions. Intriguingly, at low $[Ca^{2+}]_{free}$ values, the binding of the wild-type eNOS peptide to CaM becomes highly endothermic, the increase in entropy increases >4-fold, and its affinity for CaM increases slightly (K_d = 0.2 μM). A similar result showing a switch from an exothermic to an endothermic interaction has been reported for the binding of the nNOS CaM target domain to CaM by simply changing the experimental conditions going from a higher to a lower temperature.[37] The ΔH under at 225 nM calcium is now positive and unfavorable for binding. The change in enthalpy is compensated by a positive ΔS much larger than that observed for the wild-type peptide binding in excess calcium. In contrast, the binding of eNOSpThr495 to CaM at these low $[Ca^{2+}]_{free}$ values becomes negligible (Figure 6). This is consistent with our fluorescence experiments showing no apparent binding under these conditions. In essence, these results indicate that nonphosphorylated eNOS is more sensitive to ambient cellular Ca^{2+}, and phosphorylation serves as an attenuator of the Ca^{2+}-CaM regulation of eNOS.

We set out to understand how phosphorylation of a single residue in the CaM target domain results in diminished NOS enzyme activity. Previous studies had shown that an eNOS enzyme carrying a T495D phosphomimetic mutation binds very weakly to CaM. In contrast, the control T495A mutant showed strong binding to CaM.[15] Enzyme studies also showed that only phosphorylation of T495 or the T495D mutation resulted in a loss of eNOS enzyme activity. It had been postulated that phosphorylation of T495 reduces output by hindering the association of CaM with its binding site.[31] Until now, there had not been a structural study using a phosphorylated T495 residue. Our solution structure shows that in the presence of excess calcium, phosphorylation does not prevent the binding of CaM to the phosphorylated peptide. While the exact mechanism of how phosphorylation of Thr495 in eNOS adversely affects the activation of the enzyme is still unknown, a careful look at the complex does provide some idea of the reported cause for the reduced enzyme activity. A comparison of the two structures in Figures 1 and 2 shows that the most significant changes in the pThr495 solution structure involved two CaM amino acids, E7 and E127. In addition, both E11 and M124 are found to be in the proximity of the pThr495 phosphate group. The previously reported crystal structure of CaM bound to the human eNOS peptide shows that the side chains of these amino acids are in contact with a number of amino acids in the eNOS peptide.[31] Both E7 and E11 are part of helix A of EF hand 1 in CaM. The E7 side chain is in contact with eNOS residues K497 and E498 and has ionic interactions with R492. The E11 side chain is in contact with eNOS residues E498, A502, and I505 and has a hydrogen bond with N501. Our results shown in Figure 3 indicate that helix A is pushed away from the peptide likely because of electrostatic repulsion.

dx.doi.org/10.1021/bi401466s | *Biochemistry* 2014, 53, 1241−1249

The M124 and E127 residues are both in helix G of EF hand 4 in CaM. The side chain of M124 is in contact with eNOS residues T495, F496, and V499. Residue E127 of CaM makes contact with T495 and K497. In addition, E127 forms ionic interactions with K493 and the backbone of T496. Electrostatic repulsion could again account for the displacement of helix G of EF hand 4 from the peptide (Figure 3). Looking closely at the Delphi image with the phosphate present, we found the phosphorylation of Thr495 adds a negative charge that is close to helix G (Figure 4). The displacement of helices A and G may not be significant under conditions with 1 mM calcium, but at physiological low calcium concentration, a more significant displacement of these helices may have a detrimental effect on enzyme binding and activation. This comes from our dansyl-CaM experiments showing that the pThr495 peptide required significantly higher concentrations of calcium to bind to CaM. Our calorimetric study also showed a lack of binding of CaM to the phosphorylated peptide in the presence of 225 nM free calcium. We used TFE to induce α-helical formation and used spectropolarimetry to monitor the changes in the secondary structure of the two eNOS peptides. The secondary structure of both peptides plateaus in 30% TFE, but phosphorylation appears to result in a decrease in the degree of α-helical structure in the peptide. In the presence of high calcium concentrations, the solution structure shows that both peptides form an α-helical structure when bound to CaM.

In summary, the interactions of CaM with the peptides based on the eNOS CaM-binding domain or the eNOS CAM-binding domain phosphorylated at Thr495 are very similar at saturating Ca^{2+} concentrations. This is confirmed by our NMR spectroscopy (see Figure S2 of the Supporting Information), fluorescence, and ITC results. At the lower Ca^{2+} concentration of 225 nM, near physiological Ca^{2+} levels, no significant binding of CaM to the eNOSpThr495 peptide is observed by either method, whereas CaM is binding to nonphosphoryated eNOS. When Thr495 is phosphorylated, our results indicate there is a diminished propensity for the formation of an α-helix by the peptide in combination with electrostatic repulsion that may account for the diminished CaM-dependent activation of the eNOS enzyme at low physiological calcium concentrations.

■ ASSOCIATED CONTENT

Supporting Information

^{15}N-double-filtered NOESY spectrum of CaM with the eNOSpThr495 peptide bound, overlay of $^{1}H-^{15}N$ HSQC spectra of CaM and the CaM−eNOS peptide complex at 225 nM free Ca^{2+}, and overlay of $^{1}H-^{15}N$ HSQC spectra of CaM and the CaM−eNOSpThr495 peptide complex at 225 nM free Ca^{2+}. This material is available free of charge via the Internet at http://pubs.acs.org.

■ AUTHOR INFORMATION

Corresponding Author

*Department of Chemistry, University of Waterloo, 200 University Ave. W., Waterloo, ON N2L3G1, Canada. E-mail: tdieckma@uwaterloo.ca. Fax: (519) 746-0435. Telephone: (519) 888-4567.

Funding

This work was supported by the National Science and Engineering Research Council (NSERC) via Grants 326911-2009 and 183521.

Notes

The authors declare no competing financial interest.

■ ACKNOWLEDGMENTS

Molecular graphics images were produced using the UCSF Chimera package from the Resource for Biocomputing, Visualization, and Informatics at the University of California, San Francisco. Delphi is supported by National Science Foundation Grant DBI-9904841.

■ ABBREVIATIONS

NOS, nitric oxide synthase; iNOS, inducible NOS; eNOS, endothelial NOS; nNOS, neuronal NOS; cNOS, constitutive NOS; CaM, calmodulin; NMR, nuclear magnetic resonance; CaM−eNOS, CaM−eNOS-binding domain peptide complex; CaM−eNOSpThr495, CaM−eNOS-binding domain peptide complex with phosphorylated Thr495; PDB, Protein Data Bank; rmsd, root-mean-square deviation; NOE, nuclear Overhauser enhancement; NOESY, nuclear Overhauser effect spectroscopy; TOCSY, total correlation spectroscopy; HSQC, heteronuclear single-quantum coherence; ITC, isothermal titration calorimetry; CD, circular dichroism; TFE, trifluoroethanol.

■ REFERENCES

(1) Alderton, W. K., Cooper, C. E., and Knowles, R. G. (2001) Nitric oxide synthases: Structure, function and inhibition. *Biochem. J. 357*, 593−615.

(2) Daff, S. (2010) NO synthase: Structures and mechanisms. *Nitric Oxide 23*, 1−11.

(3) Welland, A., and Daff, S. (2010) Conformation-dependent hydride transfer in neuronal nitric oxide synthase reductase domain. *FEBS J. 277*, 3833−3843.

(4) Ikura, M., and Ames, J. B. (2006) Genetic polymorphism and protein conformational plasticity in the calmodulin superfamily: Two ways to promote multifunctionality. *Proc. Natl. Acad. Sci. U.S.A. 103*, 1159−1164.

(5) Persechini, A., and Kretsinger, R. H. (1988) The central helix of calmodulin functions as a flexible tether. *J. Biol. Chem. 263*, 12175−12178.

(6) Spratt, D. E., Israel, O. K., Taiakina, V., and Guillemette, J. G. (2008) Regulation of mammalian nitric oxide synthases by electrostatic interactions in the linker region of calmodulin. *Biochim. Biophys. Acta 1784*, 2065−2070.

(7) Spratt, D. E., Newman, E., Mosher, J., Ghosh, D. K., Salerno, J. C., and Guillemette, J. G. (2006) Binding and activation of nitric oxide synthase isozymes by calmodulin EF hand pairs. *FEBS J. 273*, 1759−1771.

(8) Spratt, D. E., Taiakina, V., Palmer, M., and Guillemette, J. G. (2007) Differential binding of calmodulin domains to constitutive and inducible nitric oxide synthase enzymes. *Biochemistry 46*, 8288−8300.

(9) Fleming, I., and Busse, R. (2003) Molecular mechanisms involved in the regulation of the endothelial nitric oxide synthase. *Am. J. Physiol. 284*, R1−R12.

(10) Piazza, M., Futrega, K., Spratt, D. E., Dieckmann, T., and Guillemette, J. G. (2012) Structure and Dynamics of Calmodulin (CaM) Bound to Nitric Oxide Synthase Peptides: Effects of a Phosphomimetic CaM Mutation. *Biochemistry 51*, 3651−3661.

(11) Fleming, I., Bauersachs, J., Fisslthaler, B., and Busse, R. (1998) Ca^{2+}-Independent Activation of the Endothelial Nitric Oxide Synthase in Response to Tyrosine Phosphatase Inhibitors and Fluid Shear Stress. *Circ. Res. 82*, 686−695.

(12) Michell, B. J., Chen, Zp., Tiganis, T., Stapleton, D., Katsis, F., Power, D. A., Sim, A. T., and Kemp, B. E. (2001) Coordinated control of endothelial nitric-oxide synthase phosphorylation by protein kinase

C and the cAMP-dependent protein kinase. *J. Biol. Chem. 276*, 17625−17628.
(13) Harris, M. B., Ju, H., Venema, V. J., Liang, H., Zou, R., Michell, B. J., Chen, Z. P., Kemp, B. E., and Venema, R. C. (2001) Reciprocal phosphorylation and regulation of endothelial nitric-oxide synthase in response to bradykinin stimulation. *J. Biol. Chem. 276*, 16587−16591.
(14) Kou, R., Greif, D., and Michel, T. (2002) Mechanisms of Signal Transduction: Dephosphorylation of Endothelial Nitric-oxide Synthase by Vascular Endothelial Growth Factor: Implications for the Vascular Responses to Cyclosporin A. *J. Biol. Chem. 277*, 29669−29673.
(15) Fleming, I., Fisslthaler, B., Dimmeler, S., Kemp, B. E., and Busse, R. (2001) Phosphorylation of Thr495 Regulates Ca^{2+}/Calmodulin-Dependent Endothelial Nitric Oxide Synthase Activity. *Circ. Res. 88*, e68−e75.
(16) Tran, Q.-K., Leonard, J., Black, D. J., and Persechini, A. (2008) Phosphorylation within an autoinhibitory domain in endothelial nitric oxide synthase reduces the Ca^{2+} concentrations required for calmodulin to bind and activate the enzyme. *Biochemistry 47*, 7557−7566.
(17) Matsubara, M. (2003) Regulation of Endothelial Nitric Oxide Synthase by Protein Kinase C. *J. Biochem. 133*, 773−781.
(18) Kolluru, G. K., Siamwala, J. H., and Chatterjee, S. (2010) eNOS phosphorylation in health and disease. *Biochimie 92*, 1186−1198.
(19) Keller, R. (2005) *Optimizing the Process of Nuclear Magnetic Resonance Spectrum Analysis and Computer Aided Resonance Assignment*, Swiss Federal Institute of Technology, Zurich.
(20) Grzesiekt, S., and Bax, A. (1992) Correlating Backbone Amide and Side Chain Resonances in Larger Proteins by Multiple Relayed Triple Resonance NMR. *J. Am. Chem. Soc. 114*, 6291−6293.
(21) Muhandiram, D. R., and Kay, L. E. (1994) Gradient-enhanced triple-resonance 3-dimensional NMR experiments with improved sensitivity. *J. Magn. Reson. 103*, 203−216.
(22) Bax, A., Clore, M., and Gronenborn, A. M. (1990) ^{1}H-^{1}H Correlation via Isotropic Mixing of ^{13}C: A New Three-Dimensional Approach for Assigning ^{1}H and ^{13}C Spectra of ^{13}C-Enriched Proteins. *J. Magn. Reson. 88*, 425−431.
(23) Ikura, M., and Bax, A. (1992) Isotope-Filtered 2D NMR of a Protein-Peptide Complex Study of a Skeletal Muscle MLCK Fragment Bound to Calmodulin. *J. Am. Chem. Soc. 114*, 2433−2440.
(24) Clore, G. M., and Gronenborn, A. M. (1991) Applications of three- and four-dimensional heteronuclear NMR spectroscopy to protein structure determination. *Prog. Nucl. Magn. Reson. Spectrosc. 23*, 43−92.
(25) Fesik, S. W., and Zuiderweg, E. R. P. (1990) Heteronuclear 3-Dimensional NMR Spectroscopy of Isotopically Labelled Biological Macromolecules. *Q. Rev. Biophys. 23*, 97−131.
(26) Shen, Y., Delaglio, F., Cornilescu, G., and Bax, A. (2009) TALOS+: A hybrid method for predicting protein backbone torsion angles from NMR chemical shifts. *J. Biomol. NMR 44*, 213−223.
(27) Brunger, A. T., Adams, P. D., Clore, G. M., Delano, W. L., Gros, P., Grosse-kunstleve, R. W., Jiang, J., Kuszewski, J., Nilges, M., Pannu, N. S., Read, R. J., Rice, L. M., Simonson, T., and Gregory, L. (1998) Crystallography & NMR System: A New Software Suite for Macromolecular Structure Determination. *Acta Crystallogr. D54*, 905−921.
(28) Pettersen, E. F., Goddard, T. D., Huang, C. C., Couch, G. S., Greenblatt, D. M., Meng, E. C., and Ferrin, T. E. (2004) UCSF Chimera: A Visualization System for Exploratory Research and Analysis. *J. Comput. Chem. 25*, 1605−1612.
(29) Kincaid, R. L., Vaughan, M., Osborne, J. C., and Tkachuk, V. A. (1982) Ca^{2+}-dependent interaction of 5-dimethylaminonaphthalene-1-sulfonyl-calmodulin with cyclic nucleotide phosphodiesterase, calcineurin, and troponin I. *J. Biol. Chem. 257*, 10638−10643.
(30) Chen, R. F. (1968) Dansyl Labeled Proteins: Determination of Extinction Coefficient and Number of Bound Residues with Radioactive Dansyl Chloride. *Anal. Biochem. 25*, 412−416.
(31) Aoyagi, M., Arvai, A. S., Tainer, J. A., and Getzoff, E. D. (2003) Structural basis for endothelial nitric oxide synthase binding to calmodulin. *EMBO J. 22*, 766−775.
(32) Broncel, M., Wagner, S. C., Paul, K., Hackenberger, C. P. R., and Koksch, B. (2010) Towards understanding secondary structure transitions: Phosphorylation and metal coordination in model peptides. *Org. Biomol. Chem. 8*, 2575−2579.
(33) Johnson, J. D., and Wittenauer, L. A. (1983) A fluorescent calmodulin that reports the binding of hydrophobic inhibitory ligands. *Biochem. J. 211*, 473−479.
(34) Mori, M., Konno, T., Ozawa, T., Murata, M., Imoto, K., and Nagayama, K. (2000) Novel Interaction of the Voltage-Dependent Sodium Channel (VDSC) with Calmodulin: Does VDSC Acquire Calmodulin-Mediated Ca^{2+}-Sensitivity? *Biochemistry 39*, 1316−1323.
(35) Censarek, P., Beyermann, M., and Koch, K.-W. (2002) Target recognition of apocalmodulin by nitric oxide synthase I peptides. *Biochemistry 41*, 8598−8604.
(36) Vorherr, T., Knöpfel, L., Hofmann, F., Mollner, S., Pfeuffer, T., and Carafoli, E. (1993) The calmodulin binding domain of nitric oxide synthase and adenylyl cyclase. *Biochemistry 32*, 6081−6088.
(37) Yamniuk, A. P., and Vogel, H. J. (2005) Structural Investigation into the Differential Target Enzyme Regulation Displayed by Plant Calmodulin Isoforms. *Biochemistry 44*, 3101−3111.
(38) Censarek, P., Beyermann, M., and Koch, K.-W. (2004) Thermodynamics of apocalmodulin and nitric oxide synthase II peptide interaction. *FEBS Lett. 577*, 465−468.